PHYSICAL REVIEW B **72**, 081406(R) (2005)

Order-disorder transition in the surface charge-density-wave phase of Cu(001)-$c(4\times4)$-In

S. Hatta, H. Okuyama, and T. Aruga*
Department of Chemistry, Graduate School of Science, Kyoto University, Kyoto 606-8502, Japan

O. Sakata
Materials Science, Japan Synchrotron Radiation Research Institute / SPring-8, Kouto, Mikazuki, Sayo-gun, Hyogo 679-5198, Japan
(Received 18 April 2005; revised manuscript received 20 June 2005; published 23 August 2005)

We have investigated the x-ray critical scattering from In/Cu(001) near the charge-density-wave phase transition. The critical exponents of the temperature dependence of the order parameter, the susceptibility, and the correlation length of the order parameter fluctuations are in agreement with those expected for a two-dimensional Ising-type phase transition. The lattice transition temperature, T_{cl}=345 K, is 60 K lower than that for the electronic transition reported recently. The surface phase transition in this system is not well described by conventional weak- or strong-coupling theories, which assume a single characteristic energy gap. It is suggested that the electronic and lattice degrees of freedom on the surface are governed separately by two different energy gaps.

DOI: 10.1103/PhysRevB.72.081406 PACS number(s): 68.35.Rh, 71.45.Lr, 61.10.−i

In recent years, considerable attention has been paid to charge-density-wave (CDW) phase transitions on surfaces and much effort has been devoted to understanding the nature of the surface phase transitions anticipated as CDW transitions.[1–6] Static properties such as geometric and electronic structures of low-temperature (LT) and high-temperature (HT) phases have been extensively studied for these phase transitions. In order to understand the mechanism of the phase transitions, the measurement of the temperature dependence of the order parameter and its fluctuations can play a decisive role. Mean-field theory for weak-coupling CDW (WCDW), which is driven by electronic entropy, predicts BCS-like behavior for both electronic and lattice order parameters, the former corresponding to the CDW energy gap and the latter to the lattice distortion amplitude. Strong-coupling CDW (SCDW) phase transitions, which are characterized by a large zero-temperature CDW gap, should be associated with an order-disorder phase transition at a temperature much lower than that for the electronic phase transition and would give rise to a characteristic behavior of the structural order parameters.[7–11]

The phase transition between the LT $c(4\times4)$ and the HT $p(2\times2)$ phases on Cu(001) covered with 0.63 monolayer (ML) of indium is associated with the formation, in the LT phase, of an electronic energy gap across the Fermi level (E_F) at k corresponding to $c(4\times4)$ surface Brillouin-zone (SBZ) boundaries, which disappears in the HT phase.[12] This indicates that the phase transition is essentially a CDW phase transition driven by the nesting of the two-dimensional (2D) Fermi contour constituted by an In-induced surface resonance band. We recently reported on a detailed angle-resolved photoelectron-spectroscopy (ARPES) study on the temperature dependence of the CDW energy gap during the phase transition.[13] While the CDW energy gap at low temperatures is as large as ~860 meV, indicative of a SCDW regime, its temperature dependence showed a behavior much similar to that expected for WCDW with the electronic transition temperature T_{ce} of 405 K. It was suggested that electronic energy and entropy play a significant role in the phase transition, as is assumed for WCDW.

On the other hand, the HT $p(2\times2)$ phase was found to be associated with a type of structural disorder by nature,[12] based on which the phase transition was suggested to be driven cooperatively by electronic and lattice entropies. In order to understand the mechanism of the phase transition, it is inevitable for us to study the details of the structural disorder in the HT phase and its relation with the change observed in the electronic structure. A model composed of coexisting antiphase domains was proposed for the disordered $p(2\times2)$ phase,[12] which is consistent with the structure model of the $c(4\times4)$ phase based on scanning-tunneling microscopy[12] (STM), low-energy electron diffraction[15] (LEED) and x-ray diffraction.[16] According to this model for the disorder, it is expected that an order-disorder transition classified into a 2D Ising universality class[14] takes place. While LEED profiles were monitored during the phase transition in the previous work,[12] the limited k resolution of LEED prevented the detailed analysis of the phase transition mechanism. In the present work, we measured the temperature dependence of the diffraction profiles by grazing-incidence x-ray diffraction, which has a k resolution (~0.003 Å^{-1}) smaller by a factor of ~30 than that of LEED. This enabled us to determine unambiguously the lattice order-disorder transition temperature, T_{cl}, and the universality class. The result, together with the previous one on the electronic transition,[13] points to the scenario for the surface CDW transition governed by two characteristic energy gaps.

The experiment was performed in an ultrahigh vacuum chamber that was mounted on a (2+2)-type diffractometer at BL13XU of SPring-8.[17] The x-ray wavelength of 0.62 Å was used. The horizontal and perpendicular slit widths were set to 0.1 mm. The reciprocal-space coordinate (hkl) is indicated below with respect to a bulk cubic unit cell, and the h direction is defined to be parallel to the [100] direction. Grazing-incidence geometry with an incidence angle of 1.5° was used to measure the diffraction profiles at l=0.3. We used a scintillation counter with Soller slits.

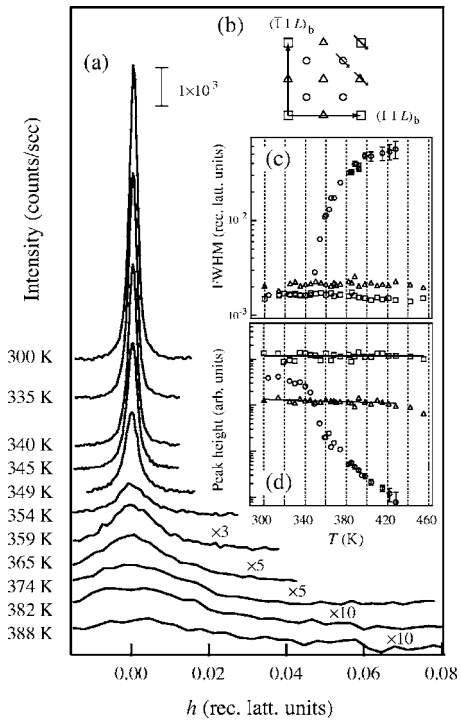

FIG. 1. (a) The quarter-order spot profiles at various temperatures in the transition region. (b) A schematic view of a $c(4\times4)$ diffraction pattern. The surface unit vectors are related to the bulk ones as $(1\ 0)_s=(1\ 1\ 0)_b$ and $(0\ 1)_s=(\bar{1}\ 1\ 0)_b$. Integer-, half-, and quarter-order spots in the surface notation are marked with, □, △, and ○, respectively. Short arrows indicate the scan directions. The temperature dependence of FWHM (c) and height (d) for the measured profiles are shown, where the markers correspond to those in (b).

The Cu(001) sample with a diameter of 10 mm was oriented paralled to the (001) plane within ±0.2°. The sample cleaning was achieved by repeated cycles of Ar ion sputtering at 550 eV and annealing at 800 K. Indium was evaporated from an alumina crucible located in front of the surface at a distance of ~30 mm. Sharp $c(4\times4)$ LEED patterns were obtained over the entire surface by the procedure reported in the previous work.[13] The sample temperature was controlled with a filament behind the sample and measured with a thermocouple in contact with a Ta ring attached to the sample side. The sample temperatures were maintained within ±1 K during the measurement of each profile.

Figure 1(b) shows a schematic view of a $c(4\times4)$ diffraction pattern. We measured profiles along the h direction centering at $(hkl)=(0\ 2\ 0.3)$, $(0.5\ 1.5\ 0.3)$, and $(0\ 1.5\ 0.3)$, which correspond, in the LEED notation, to an integer-, a half-, and a quarter-order spot, respectively. The temperature dependence of the quarter-order spot profile is shown in Fig. 1(a). At 300 K, the profile was very sharp and its full width at half maximum (FWHM) of 0.0017 reciprocal lattice units (r.l.u.) corresponds to a domain size as large as 2000 Å. Upon elevating the temperature, the profile was broadened rapidly above 350 K and the integrated intensity was reduced gradually. The profile was recorded up to 430 K, where the width was ~0.05 r.l.u.

Figures 1(c) and 1(d) show the temperature dependence of the height and FWHM of the measured profiles. In contrast to the quarter-order spot, the shape of the integer- and half-order spot profiles was mostly unchanged in 300–460 K. The gradual decrease of the peak heights is well fitted by using the Debye-Waller (DW) factors as shown by straight lines. The DW factors are determined as 0.0028 and 0.0043 K^{-1} for the integer- and half-order spots, respectively. On the other hand, we also estimated the DW factor from the temperature dependence of background intensity. This yielded 0.0014 K^{-1}, which is close to the value for a bulk Cu crystal. The difference in the DW factors indicates the enhancement of thermal lattice vibration at the surface. We used the DW factor of 0.0043 K^{-1} in the analysis of the quarter-order spot intensity.

A total scattering intensity $S(q,t)$, which consists of contributions of the Bragg diffraction (long-range order; LRO) and the critical fluctuation (short-range order; SRO), is represented by

$$S(q,T)=I_{long}(T)F(q)+F_{SRO}(q,T)+I_{bg}. \tag{1}$$

I_{long} denotes the temperature dependence of the Bragg diffraction term and corresponds to the square of the order parameter (magnetization) for $T<T_{cl}$. $F(q)$ is due to an instrument function and the finite domain size at low temperatures. I_{bg} denotes the background intensity. For the shape of diffuse scattering term F_{SRO}, based on the assumption of exponential distribution of domain size, a Lorentz function

$$F_{SRO}(q,T)=\frac{\chi(T)}{1+q^2\xi^2(T)}, \tag{2}$$

is applied, where χ and ξ represent the susceptibility and the correlation length, respectively, of the order parameter fluctuations. According to the critical scattering theory, the three parameters, I_{long}, χ, and ξ, are scaled to power laws of the reduced temperature, $t=(T-T_{cl})/T_{cl}$, as $I_{long}\propto|t|^{2\beta}$, $\chi\propto|t|^{-\gamma}$ and $\xi\propto|t|^{-\nu}$.

The quarter-order spot profile in 300–340 K is represented well by a single Lorentz function with a constant width, as shown in Figure 2(a), indicating that the SRO component is negligible. According to Eq. (1), this profile shape represents $F(q)$ and its height corresponds to I_{long}. Above 340 K, the profile becomes broader as shown in Fig. 1. The profile at 345 K is fitted with Eq. (1) as shown in Fig. 2(b), which shows that the LRO and SRO components have comparable magnitudes. At higher temperatures, the profile gets further broader and the fitting shows a negligible contribution of the LRO component above 345 K. The Lorentz-type profiles were observed up to 430 K.

The temperature dependence of I_{long}, χ, and ξ are plotted as a function of temperature in Fig. 3. In Fig. 3(c), ξ^{-1}, which corresponds to the FWHM of the SRO components, is also shown, which is well fitted with a straight line, particularly at temperatures below ~380 K. This directly indicates $\nu=1$, which is expected for the 2D Ising universality class. We determined $T_c=345\pm2$ K based on the fitting of the straight line for ξ^{-1}. We estimated the critical exponents by fitting the power-law functions to the data. This gave $\beta=0.15\pm0.19$,

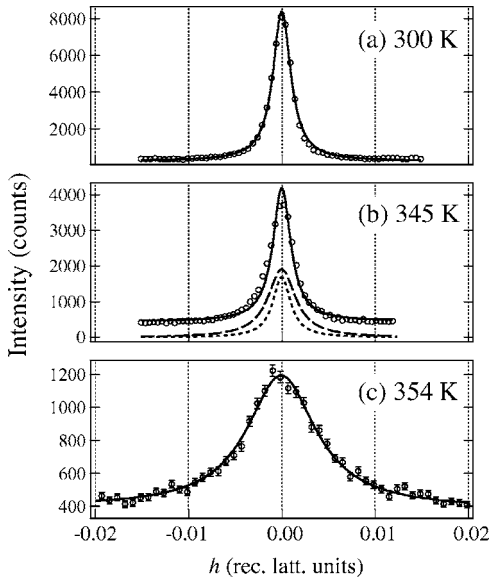

FIG. 2. Examples of the profile analysis. The solid lines are the fitting function for the total scattering intensity. The dotted and dashed lines represent the LRO and SRO components, respectively. Statistical error bars are not shown when smaller than symbol size. Each point was acquired with a dwell time of 1 s.

$\gamma=1.36\pm0.62$ and $\nu=1.14\pm0.27$. These values agree, within error, with the theoretical values, $\beta=0.125$, $\gamma=1.75$, $\nu=1$, for the 2D Ising model, but are inconsistent with the exponents of the mean-field model, $\beta=0.5$, $\gamma=1$, $\nu=0.5$. The solid curves in Fig. 3 are the power-law curves with the theoretical values for the 2D Ising model. The theory and the experiment show a good agreement in a significantly wide

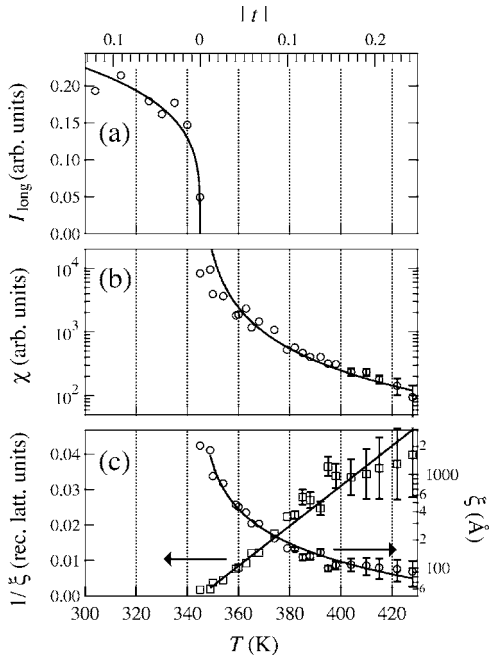

FIG. 3. The temperature dependences of I_{long}, χ, and ξ. The solid lines are theoretical curves using $\beta=1/8$, $\gamma=7/4$, and $\nu=1$ for the 2D Ising universality class. ξ^{-1} is also shown (□) in the bottom panel.

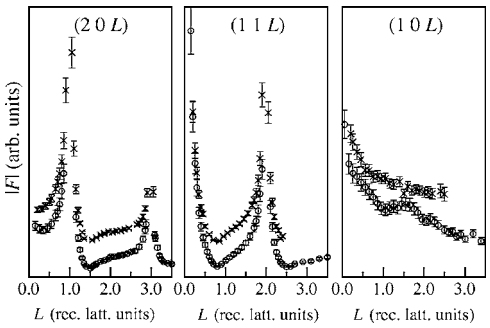

FIG. 4. CTRs at $(hk)=(2\ 0)$ and $(1\ 1)$ and a half-order superstructure rod at $(hk)=(1\ 0)$ for the LT (○) and HT (×) phases.

temperature range. We therefore conclude that the phase transition is classified into the 2D Ising universality class. This indicates that an 2D order-disorder transition occurs, as suggested in the previous work.[12] Note that, in principle, χ and ξ should exhibit divergence at T_{cl}. In real systems, however, they are suppressed because of the finite-size effect. The data within 5 K from T_{cl} were therefore excluded in the fitting procedure. On the other hand, the power-law dependence of ξ is justified under the condition that the correlation length ξ is significantly larger than a lattice constant a. The observed correlation length is larger than ~100 Å at around 400 K, which fulfills the above condition.

Figure 4 shows crystal truncation rods (CTRs), $(2\ 0\ L)$ and $(1\ 1\ L)$, and a half-order superstructure rod, $(1\ 0\ L)$, for the HT and LT phases, which were measured at 25 and 455 K, respectively. The overall L dependence for HT and LT phases are similar, which indicates that the local structure within the $p(2\times2)$ unit cell is mostly unchanged between the LT and HT phases. This has also been suggested in the LEED work based on the agreement of the I-V curves from the two phases,[12] and supports the model that the HT phase has a disordered nature.

The present result corroborates our understanding to this surface CDW. As was found in the ARPES work,[13] the surface resonance band relevant to the CDW formation has a large energy gap $2\Delta=860$ meV at the $c(4\times4)$ SBZ boundary. According to the approximate relation between the CDW energy gap size, 2Δ, and the coherence length of the CDW wave functions,[18] $\hbar v_F/\pi\Delta$, where v_F denotes the Fermi velocity, the coherence length is estimated to be ~8 Å, where the free electron mass is assumed. This value is comparable to the $c(4\times4)$ lattice constant of 7.23 Å, and leads to a rather localized chemical-bond picture for SCDW as suggested by McMillan.[7] In such a case, the mean-field theory predicts very high transition temperature (>1000 K) and it is expected that a lattice order-disorder transition sets in at a much lower temperature.

For SCDW, the CDW phase fluctuation effect becomes important below the mean-field transition temperature. This can be described by introduction of a complex CDW order parameter in the Landau theory. When the CDW phase correlation length is shortened through the lattice entropy as temperature increases, the CDW order parameter magnitude $|\Delta|$ is no longer linearly connected to the lattice long-range order parameter. The order-disorder transition observed in

the present work certainly represent such a disappearance of the spatial CDW phase correlation, because the CDW energy gap remains finite above 345 K as reported in the ARPES work.[13]

On the other hand, the temperature dependence of the surface band structure has been revealed to exhibit characteristic change near E_F. At low temperatures, the upper edge of the energy gap is located closer to E_F than the lower edge. Because the electrons in the bulk bands at E_F can be thermally excited to the unoccupied surface-band states, the electronic entropy contribution to the free energy should be estimated by the "energy gap" δ, which is defined by the energy difference between the upper edge of the energy gap and E_F. The obtained value of δ was $\sim$230 meV, which is about half as large as that of Δ.

In this surface system, the condensation enthalpy of CDW is dominated by the surface-band energy gap 2Δ, while the electronic entropy is governed by the energy δ and hence the electronic transition occurs at a temperature much lower than that expected from 2Δ. This results in successive occurence of the lattice order-disorder and electronic gapped-ungapped transitions at a close temperature interval. It is emphasized that such a scenario would be valid also for other multiband systems in surfaces, bulk materials, and nanostructures.

It would be expected that the lattice order-disorder transition yields an anomaly in the $\Delta(T)$ data. A weak undulation at 320–370 K in the $\Delta(T)$ curve shown in Fig. 4 of Ref. 13 might correspond to such an anomaly. Further precise measurement is needed for unambiguous discussion. On the other hand, the electronic transition at T_{ce}=405 K should have an effect on the temperature dependence of the lattice order parameter. In Fig. 3(c), it seems that the increase of $1/\xi$ becomes moderate above $\sim$400 K. Although this temperature may exceed the range where the scaling hypothesis is valid, we note the possibility that the observed change is caused by the structural change associated with the electronic transition. The knowledge on the structural change should be obtained from differences between reciprocal rods from the two phases. A slight difference seen in the (1 0 L) rod might be due to the structural change within the $p(2\times2)$ unit cell. However, because of difficulties in the structure analysis of fluctuating surfaces, quantitative argument cannot be made at the moment.

This work was supported in part by the Kyoto University Alliance for Chemistry (a COE program of the Ministry of Education, Culture, Sports, Science, and Technology, Japan). The synchrotron radiation experiments were performed at SPring-8 with the approval of the Japan Synchrotron Radiation Research Institute (JASRI) as a Nanotechnology Support Project of the Ministry of Education, Culture, Sports, Science and Technology. (Proposals No. 2002B0336-ND1-np and 2003A0237-ND1-np/BL13XU)

*Electronic address: aruga@kuchem.kyoto-u.ac.jp

[1] J. M. Carpinelli, H. H. Weitering, E. W. Plummer, and R. Stumpf, Nature (London) **381**, 398 (1996).

[2] J. M. Carpinelli, H. H. Weitering, M. Bartkowiak, R. Stumpf, and E. W. Plummer, Phys. Rev. Lett. **79**, 2859 (1997).

[3] H. W. Yeom, S. Takeda, E. Rotenberg, I. Matsuda, K. Horikoshi, J. Schaefer, C. M. Lee, S. D. Kevan, T. Ohta, T. Nagao, and S. Hasegawa, Phys. Rev. Lett. **82**, 4898 (1999).

[4] T. Nakagawa, G. I. Boishin, H. Fujioka, H. W. Yeom, I. Matsuda, N. Takagi, M. Nishijima, and T. Aruga, Phys. Rev. Lett. **86**, 854 (2001).

[5] K. Swamy, A. Menzel, R. Beer, and E. Bertel, Phys. Rev. Lett. **86**, 1299 (2001).

[6] J. R. Ahn, H. W. Yeom, H. S. Yoon, and I.-W. Lyo, Phys. Rev. Lett. **91**, 196403 (2003).

[7] W. L. McMillan, Phys. Rev. B **16**, 643 (1977).

[8] E. Tosatti, Solid State Commun. **25**, 637 (1978).

[9] E. Tosatti, in *Modern Trends in the Theory of Condensed Matter*, edited by A. Pekalski and J. Przystawa, Lecture Notes in Physics Vol. 115 (Springer-Verlag, Berlin, 1980) p. 501.

[10] E. Tosatti, in *Electronic Surface States and Interface States on Metallic Systems*, edited by E. Bertel and M. Donath (World Scientific, Singapore, 1995), p. 67.

[11] T. Aruga, J. Phys.: Condens. Matter **14**, 8393 (2002).

[12] T. Nakagawa, H. Okuyama, M. Nishijima, T. Aruga, H. W. Yeom, E. Rotenberg, B. Krenzer, and S. D. Kevan, Phys. Rev. B **67**, 241401(R) (2003).

[13] S. Hatta, H. Okuyama, M. Nishijima, and T. Aruga, Phys. Rev. B **71**, 041401(R) (2005).

[14] B. N. J. Persson, Surf. Sci. Rep. **15**, 1–135 (1992).

[15] K. Pussi, T. McEvoy, C. J. Barnes, A. A. Cafolla, E. AlShamaileh, and M. Lindroos, Surf. Sci. **526**, 141 (2003).

[16] S. Hatta, C. J. Walker, O. Sakata, H. Okuyama, and T. Aruga, Surf. Sci. **565**, 114 (2004).

[17] O. Sakata, Y. Furukawa, S. Goto, T. Mochizuki, T. Uruga, T. Takeshita, T. Ohashi, T. Matsushita, S. Takahashi *et al.*, Surf. Rev. Lett. **10**, 543 (2003).

[18] G. Grüner, *Density Waves in Solids* (Addison-Wesley, Reading, MA, 1994).